NTNU

TMR4240

Project - Part 2

Authors:
Shiv Jeet Rai
Shangming Li
Zhenying Wu
Kristine Elisabeth Aas Herje

November 18, 2015

Contents

Chapter 1

Executive Summary

This part of the project is an extension of the project part one. The vessel dynamics is still the center of the project. From project part one the DP controller and reference model are to be a part of the project part two. While the current given in part one are to be exchanged by a more detailed and realistic environmental forces model. Also there are to be implemented a thrust allocation part, which are to transfer the forces given by the DP controller and send it into a thrust dynamics block. In this way the vessel will respond in a more realistic way, since the applied forces are the forces that the thrusters actually can give. There will also be included noise on the feedback from the vessel to give a more realistic situation. Since there now are a more realistic representation of inputs and outputs on the vessel, there are to be designed an observer to give position and velocity to the DP controller.

After everything was implemented, a series of simulations was done. In the first simulations the different parts were allowed to work on the vessel and it was looked and compared how it behaved. When it came to the observer it was implemented two different ones, and their behavior was to be analyzed to see which of them was working best. When all of the different parts were simulated, a complete simulation of the entire system was done. In the end it was done a capability plot and tested how robust the observer was.

The results were mostly satisfactory.

Chapter 2

Detailed environmental loads

2.1 Given information

In this part of the project the environmental loads acting on the vessel hull, is to be implemented in an more accurate way. External forces, such as ice loads and mooring lines, are to be disregarded. The only environmental loads that are to be taken into account are the wind and current. To get a realistic representation, the loads have to be calculated as generalized forces on the body frame for all six degrees of freedom. The formulas to calculate this is given as:

$$F_{Wind} = |V_\omega|^2 * C_\omega(\alpha_{r\omega}) \tag{2.1}$$

$$F_{Current} = |V_c|^2 * C_c(\alpha_{rc}) \tag{2.2}$$

where:

- F_{Wind} are the generalized wind forces.
- $F_{Current}$ are the generalized current forces.
- V_ω is the wind velocity modulus.
- V_c is the current velocity modulus.
- $C_\omega(x)$ is the wind coefficient matrix
- $C_c(x)$ is the current coefficient matrix
- $\alpha_{r\omega}$ is the relative angle between the wind direction and the vessel heading.
- α_{rc} is the relative angle between the current direction and the vessel heading.

Both current and wind are to have a mean component and a slowly varying. The wind are also to have a gust component. The mean component also has a mean angle and the slowly varying are slowly varying about this angle, with a maximum distance from the mean angle on 5 degrees. The gust are not to have its one angle.

2.2 Implementation

To use the formulas 2.1 and 2.2 we need to find the absolute value of the speed of the wind and current and also the relative angle fore each of them. The way this is done is that each component of each force are decomposed in north and east direction. There, all north and east components for each force are added together respectively. In the end the absolute value of the vector are found, together with the angle of the total speed.

To go more in detail, one can start with the decomposition of the velocities in north and east direction:

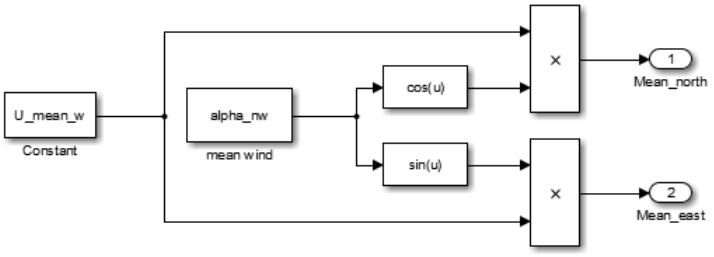

Figure 2.1: Mean Wind

As is seen in the figure 2.1 the given mean velocity are simply multiplied with the sinus and cosine of the given mean angle of the wind.

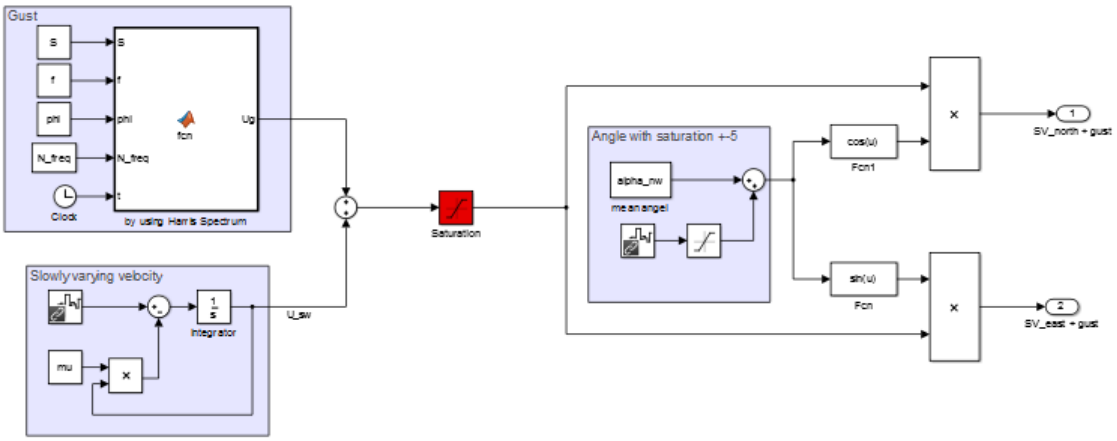

Figure 2.2: Slowly varying wind and gust

The figure 2.2 shows that the slowly varying and the gust are harder to find, but the decomposition in north and east are the same.

To find the velocity of the gust it is used a Harris Spectrum and the slowly varying wind are modeled by white noise. Since the gust does not have an angle of its own, the gust and slowly varying are simply added before one decomposes. There, the velocity are saturated to 20% of the mean value such that it does not dominate the total force. Also on the angle there are used a white noise that are saturated according to the specifications.

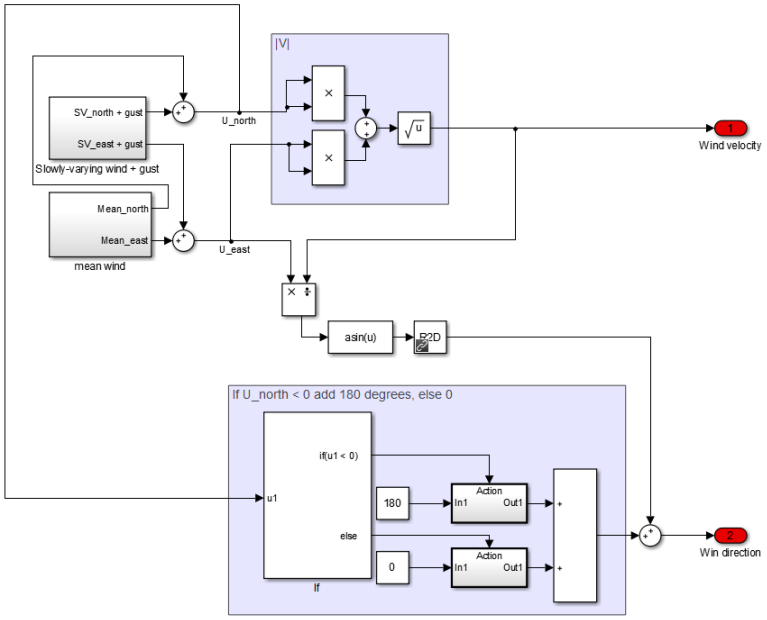

Figure 2.3: Total wind velocity and angle

In the figure 2.3 it is shown how the total, or the absolute value of the wind velocity and the angel of the wind velocity.

The velocity and angle of the current are found in the same way, except that the current does not contain gust and that the power of the slowly varying are regulated compared to the mean current velocity.

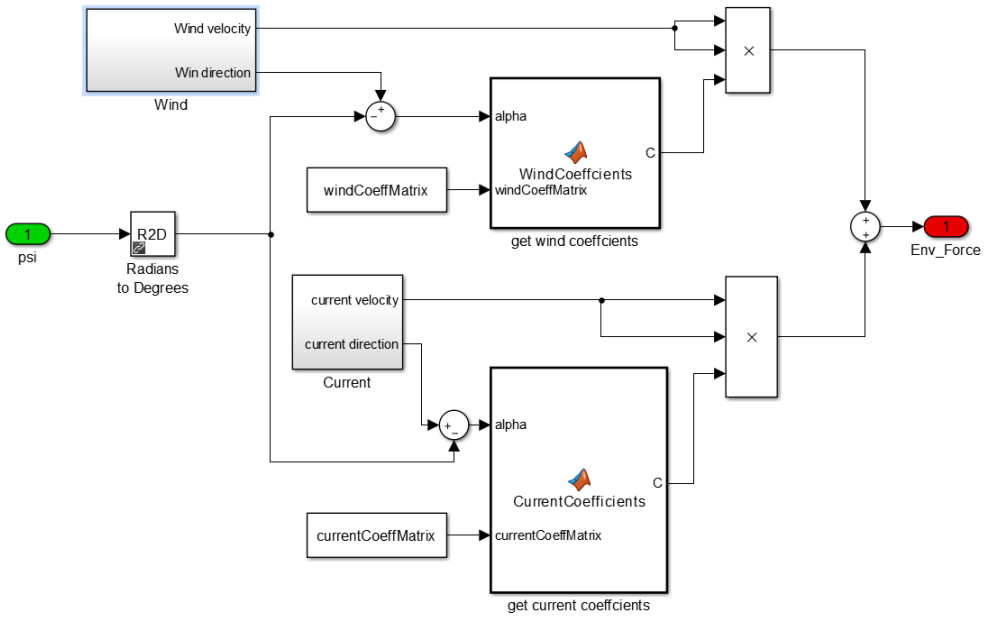

Figure 2.4: Getting the enviromental loads in six DOF

In the end the equations 2.1 and 2.2 are implemented as showed in figure 2.4

Chapter 3

Observer Implementation

3.1 Given information

The aim was to create two different observers for the system, here namely a Kalman Filter and a Nonlinear Passive Observer.

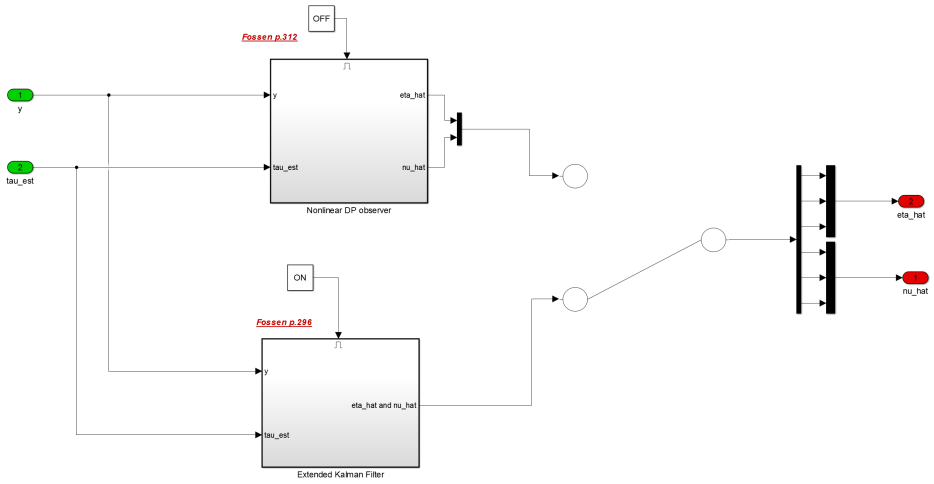

Figure 3.1: Nonlinear Passive Observer & Extended Kalman Filter

An observer's purpose is to create estimated states from given measurements and force. From Figure 3.1 it can be seen that in this project the inputs consisted of measured positions, y, and estimated generalized forces, τ. Notice that the inputs does not include velocity measurements, as the project wanted them to be estimated by the observer.

The following matrices were given:

- Mass Matrix (Rigid Body + Added Mass)

$$M = \begin{bmatrix} 7 \cdot 10^6 & 0 & 0 \\ 0 & 11 \cdot 10^6 & 0 \\ 0 & 0 & 3 \cdot 10^9 \end{bmatrix}$$

- Damping matrix:

$$D = \frac{1}{10} \cdot \begin{bmatrix} 1.7 \cdot 10^5 & 0 & 0 \\ 0 & 1.4 \cdot 10^5 & 0 \\ 0 & 0 & 5.4 \cdot 10^7 \end{bmatrix}$$

3.2 Kalman Filter

3.2.1 Observer Model

To design a Kalman filter for a DP system the following system can be used [2]:

$$\dot{\eta} = R(\psi)\nu \tag{3.1}$$
$$\dot{b} = \omega_1 \tag{3.2}$$
$$\dot{\nu} = -M^{-1}D\nu + M^{-1}R^T(\psi) + M^{-1}\tau \tag{3.3}$$
$$y = \eta + v \tag{3.4}$$
$$\tag{3.5}$$

Assumptions to this system are:

- Zero wave disturbances, $\varepsilon = 0$
- The ocean currents are compensated by using integral action. Here it is done by assuming that the ocean currents can be treated as a slowly varying bias vector in {n}, namely b. By assuming that the ocean currents are compensated and moving with low speed the Centripetal and Coriolis term, $C_{RB}(\nu)\nu + C_A(\nu_r)\nu$, can be neglected as in the system above.
- The term $-T^{-1}b \approx 0$, since it is assumed $T \approx \infty$.

Since the equations (3.1-3.5) are clearly nonlinear due to the rotation matrix $R(\psi)$, they were written as the following state-space model:

$$\begin{aligned} \dot{x} &= f(x) + Bu + Ew \\ y &= Hx + v \end{aligned} \tag{3.6}$$

It can be seen:

$$f(x) = \begin{bmatrix} R(\psi)\nu \\ 0_{3\times 3} \\ M^{-1}R(\psi)b - M^{-1}D\nu \end{bmatrix} \qquad B = \begin{bmatrix} 0_{3\times p} \\ 0_{3\times p} \\ M^{-1}B_u \end{bmatrix} \qquad E = \begin{bmatrix} 0_{3\times 3} \\ I_{3\times 3} \\ 0_{3\times 3} \end{bmatrix} \tag{3.7}$$

$$H = \begin{bmatrix} I_{3\times 3} & 0_{3\times 3} & 0_{3\times 3} \end{bmatrix} \tag{3.8}$$

where $x = \begin{bmatrix} \eta & b & \nu \end{bmatrix}^T$, $\omega = \begin{bmatrix} \omega_1 \end{bmatrix}^T$

The coloumns in matrix B in (3.7) are given by the number of states one want the force τ to influence. Since the system is a 3DOF motion p = 3, since the other states are assumed stabilized.

$$B_u = I_{3\times 3}$$

To use the (discrete) Extended Kalman Filter algorithm presented by Fossen[1]:

Discrete-time extended Kalman filter (EKF)	
Design matrices	$\boldsymbol{Q}(k) = \boldsymbol{Q}^\top(k) > 0,\ \boldsymbol{R}(k) = \boldsymbol{R}^\top(k) > 0$ (usually constant)
Initial conditions	$\bar{\boldsymbol{x}}(0) = \boldsymbol{x}_0$ $\bar{\boldsymbol{P}}(0) = E[(\boldsymbol{x}(0) - \hat{\boldsymbol{x}}(0))(\boldsymbol{x}(0) - \hat{\boldsymbol{x}}(0))^\top] = \boldsymbol{P}_0$
Kalman gain matrix	$\boldsymbol{K}(k) = \bar{\boldsymbol{P}}(k)\boldsymbol{H}^\top(k)\,[\boldsymbol{H}(k)\bar{\boldsymbol{P}}(k)\boldsymbol{H}^\top(k) + \boldsymbol{R}(k)]^{-1}$
State estimate update	$\hat{\boldsymbol{x}}(k) = \bar{\boldsymbol{x}}(k) + \boldsymbol{K}(k)\,[\boldsymbol{y}(k) - \boldsymbol{H}(k)\bar{\boldsymbol{x}}(k)]$
Error covariance update	$\hat{\boldsymbol{P}}(k) = [\boldsymbol{I} - \boldsymbol{K}(k)\boldsymbol{H}(k)]\,\bar{\boldsymbol{P}}(k)\,[\boldsymbol{I} - \boldsymbol{K}(k)\boldsymbol{H}(k)]^\top$ $+\boldsymbol{K}(k)\boldsymbol{R}(k)\boldsymbol{K}^\top(k), \quad \hat{\boldsymbol{P}}(k) = \hat{\boldsymbol{P}}(k)^\top > 0$
State estimate propagation	$\bar{\boldsymbol{x}}(k+1) = \mathcal{F}(\hat{\boldsymbol{x}}(k), \boldsymbol{u}(k))$
Error covariance propagation	$\bar{\boldsymbol{P}}(k+1) = \boldsymbol{\Phi}(k)\hat{\boldsymbol{P}}(k)\boldsymbol{\Phi}^\top(k) + \boldsymbol{\Gamma}(k)\boldsymbol{Q}(k)\boldsymbol{\Gamma}^\top(k)$

Figure 3.2: Extended Kalman Filter

The discrete linearized state-space parameters were found as:

$$\Phi = I + h\frac{\partial f(\hat{x}(k), u(k))}{\partial x(k)}|_{x(k)=\hat{x}(k)} \tag{3.9}$$

$$\Gamma \approx hE \tag{3.10}$$

$$\mathcal{F}(\hat{x}(k), u(k)) = \hat{x}(k) + h[f(\hat{x} + Bu_k)] \tag{3.11}$$

The Jacobian, $J = \frac{\partial f}{\partial x}$, was found as:

$$\begin{bmatrix} 0 & 0 & -\mathrm{s}(\psi)u - \mathrm{c}(\psi)v & 0 & 0 & 0 & \mathrm{c}(\psi) & -\mathrm{s}(\psi) & 0 \\ 0 & 0 & \mathrm{c}(\psi)u - \mathrm{s}(\psi)v & 0 & 0 & 0 & \mathrm{s}(\psi) & -\mathrm{c}(\psi) & 0 \\ 0 & 0 & 0 & 0 & 0 & 0 & 0 & 0 & 1 \\ 0 & 0 & 0 & 0 & 0 & 0 & 0 & 0 & 0 \\ 0 & 0 & 0 & 0 & 0 & 0 & 0 & 0 & 0 \\ 0 & 0 & M_{11}^{-1}\mathrm{s}(\psi)b_1 + M_{22}^{-1}\mathrm{c}(\psi)b_2 & -M_{11}^{-1}\mathrm{c}(\psi) & -M_{22}^{-1}\mathrm{s}(\psi) & 0 & (M^{-1}D)_{11} & 0 & 0 \\ 0 & 0 & M_{11}^{-1}\mathrm{c}(\psi)b_1 + M_{22}^{-1}\mathrm{s}(\psi)b_2 & -M_{11}^{-1}\mathrm{s}(\psi) & -M_{22}^{-1}\mathrm{c}(\psi) & 0 & (M^{-1}D)_{22} & 0 & 0 \\ 0 & 0 & 0 & 0 & 0 & -M_{33}^{-1} & 0 & 0 & (M^{-1}D)_{33} \end{bmatrix} \tag{3.12}$$

where $\mathrm{s}(\psi)$ and $\mathrm{c}(\psi)$ are $\sin(\psi)$ and $\cos(\psi)$ respectively. u and v are from $\nu = [u, v, r]^T$.

In addition to the state-space model some additional parameters are required. Those are:

- The covariance matrices Q and R.

$$Q = Q^T = 10^9 \cdot \begin{bmatrix} 1 & 0 & 0 \\ 0 & 1 & 0 \\ 0 & 0 & 1 \end{bmatrix} \qquad R = R^T = 10^{-4} \begin{bmatrix} 0.0115 & 0 & 0 \\ 0 & 0.0120 & 0 \\ 0 & 0 & 0.0004 \end{bmatrix}$$

  10^{-4} is just a scaling factor for the Q-R relationship.

  - How Q was tuned: To find an estimate of the matrix Q a trial and error approach was used. It is known that the Q represent the uncertainty in the states due to the noise ω. Higher values in Q will give result in higher uncertainty in the related states. In this case the Q is related to the states b and ν. Since the bias is very hard to model in the real life, it were placed high uncertainties to the states related to it. In addition one have the ratio between Q and R, thus these values for Q were found by trial and error until a satisfactory behaviour was observed.

- How R was tuned: To find an estimate of the variance of the measurement noise, only the measurement noise was simulated. This is the same as saying that the vessel kept the position at the origin perfectly if the system, therefore the deviations in the {n} were a direct result of noise induced. The deviations can be seen in Figure 3.3

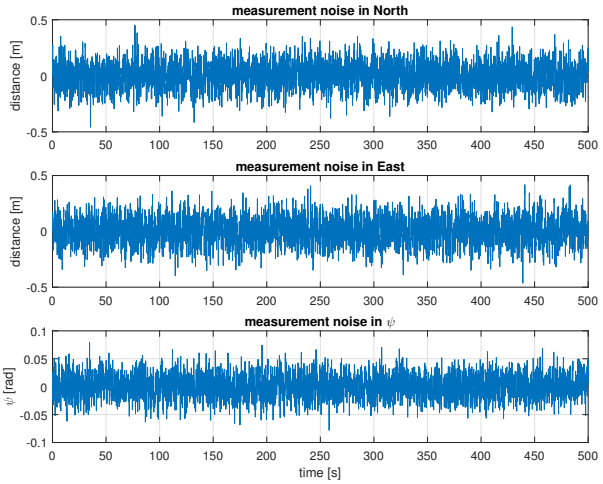

Figure 3.3: Measurement noise while the craft is at initial position (origin)

By using the MatLab function var() and the following MatLab script:

```
%eta_noise is an ToWorkSpace variable
R11 = var(eta_noise.Data(:,1));
R22 = var(eta_noise.Data(:,2));
R33 = var(eta_noise.Data(:,3));
```

$$\Rightarrow R = \text{scaling factor}\dot{R} = 10^{-4}\begin{bmatrix} 0.0115 & 0 & 0 \\ 0 & 0.0120 & 0 \\ 0 & 0 & 0.0004 \end{bmatrix}$$

- matrix $P_0 = E[(x(0) - \hat{x}(0))(x(0) - \hat{x}(0))^T] = 10^7 \cdot \begin{bmatrix} 0 & 0 & 0 & 0 & 0 & 0 & 0 & 0 & 0 \\ 0 & 0 & 0 & 0 & 0 & 0 & 0 & 0 & 0 \\ 0 & 0 & 0 & 0 & 0 & 0 & 0 & 0 & 0 \\ 0 & 0 & 0 & 1 & 0 & 0 & 0 & 0 & 0 \\ 0 & 0 & 0 & 0 & 1 & 0 & 0 & 0 & 0 \\ 0 & 0 & 0 & 0 & 0 & 1 & 0 & 0 & 0 \\ 0 & 0 & 0 & 0 & 0 & 0 & 0 & 0 & 0 \\ 0 & 0 & 0 & 0 & 0 & 0 & 0 & 0 & 0 \\ 0 & 0 & 0 & 0 & 0 & 0 & 0 & 0 & 0 \end{bmatrix}$

  - How P_0 was chosen: Due to the high uncertainty in Q due to bias, the states were set to high values such that the initial error would been taken care of faster.

- vector $x_0 = E[(x(0) - \hat{x}(0))] = \begin{bmatrix} 0 & 0 & 0 & 1 & 1 & 1 & 0 & 0 & 0 \end{bmatrix}^T$:

  - How x_0 was chosen: It was assumed that the measured states were equal to the actual states in the beginning, except for the bias. Since the P_0 were set to high values for the bias, one could have lower values for the bias here. The P_0 would take care of it.

3.2.2 Simulink

The observer was implemented through a MatLab function as seen in 3.4.

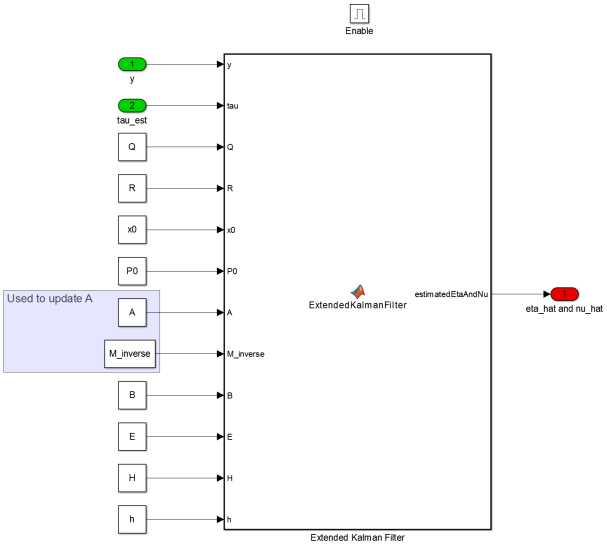

Figure 3.4: Extended Kalman Filter

The implementation can be seen in the Matlab files delivered on itsLearing.

3.3 Nonlinear Passive Observer

3.3.1 Observer Model

To design a Nonlinear Passive Observer for an DP system the following system can be used [1]:

$$\dot{\hat{\eta}} = R(\psi)\hat{\nu} + K_2\tilde{y} \tag{3.13}$$

$$\dot{\hat{b}} = K_3\tilde{y} \tag{3.14}$$

$$M\dot{\hat{\nu}} = -D\hat{\nu} + R^T(\psi) + \tau + \tau_{\text{wind}} + K_4\tilde{y} \tag{3.15}$$

$$\hat{y} = \hat{\eta} \tag{3.16}$$

where $\tilde{y} = y - \hat{y}$ and K_{2-4} are observer gain matrices to be interpreted later.

Assumptions to this system are as same for the Extended Kalman Filter. For simplicity they are repeated here:

- Zero wave disturbances, $\varepsilon = 0$
- The ocean currents are compensated by using integral action. Here it is done by assuming that the ocean currents can be treated as a slowly varying bias vector in {n}, namely b. By assuming that the ocean currents are compensated and moving with low speed the Centripetal and Coriolis term, $C_{RB}(\nu)\nu + C_A(\nu_r)\nu$, can be neglected as in the system above.
- The term $-T^{-1}b \approx 0$, since it is assumed $T \approx \infty$.

In order to use the Nonlinear Passive observer the the observer gains have to be chosen such that stability is achieved. In order to do that, they can be chosen such that they satisfy the Kalman-Yakubovich-Popov (KYP) lemma.

Thus the matrices:

$$K_2 = \text{diag}\{K_{21}, K_{22}, K_{23}\} \tag{3.17}$$

$$K_3 = \text{diag}\{K_{31}, K_{32}, K_{33}\} \tag{3.18}$$

$$K_4 = \text{diag}\{K_{41}, K_{42}, K_{43}\} \tag{3.19}$$

had to satisfy:

$$K_{2i} = \omega_{ci} \tag{3.20}$$

$$\frac{1}{T_i} \ll \frac{K_{3i}}{K_{4i}} \leq \omega_{oi} \leq \omega_{ci} \tag{3.21}$$

where ω_{ci} is the cut-off frequency of the wave, ω_{oi} is the peak frequency of the wave and T_i is the time constant.

Since the bias is supposed to counteract the environmental forces, the K_3 has to be chosen high. Due to not having waves, the wave frequency, ω_c was chosen more or less chosen randomly. It is not desirable to have a high ω_c since the system will then be more sensitive to noise. Thus it is not desirable that the frequency is very, but since a low ω_c would mean a high K_4, which would add more stiffness, the ω_c was chosen after trial and error.

It was also noted that not satisfying the KYP, $\frac{K_3}{K_4} > \omega_c$, gave better velocity. It is true that KYP lemma is more a mathematical proof and would in practice be something close. The observer gave better response when the KYP was not satisfied, however it was chosen that satisfying the KYP was important. Thus the result by the Nonlinear Passive observer was in some sense worse than what could have been achieved. The reason was to make a tuning rule for the Nonlinear Passive, but since the system did not have waves, the rules in the lecture notes do not make sense since the ω_o and ω_c are unknown.[1]

By interpreting the controller gains K_{3i} and K_{4i} as forces and moments, and K_{2i} as an damping term the resulting values were found:

$$K_2 = \begin{bmatrix} 100 & 0 & 0 \\ 0 & 100 & 0 \\ 0 & 0 & 200 \end{bmatrix} \qquad K_3 = 10^8 \cdot \begin{bmatrix} 1 & 0 & 0 \\ 0 & 1 & 0 \\ 0 & 0 & 100 \end{bmatrix} \qquad K_4 = 10^6 \begin{bmatrix} 1 & 0 & 0 \\ 0 & 1 & 0 \\ 0 & 0 & 100 \end{bmatrix} \tag{3.22}$$

3.3.2 Simulink

The observer was implemented through Simulink as seen in figure 3.5.

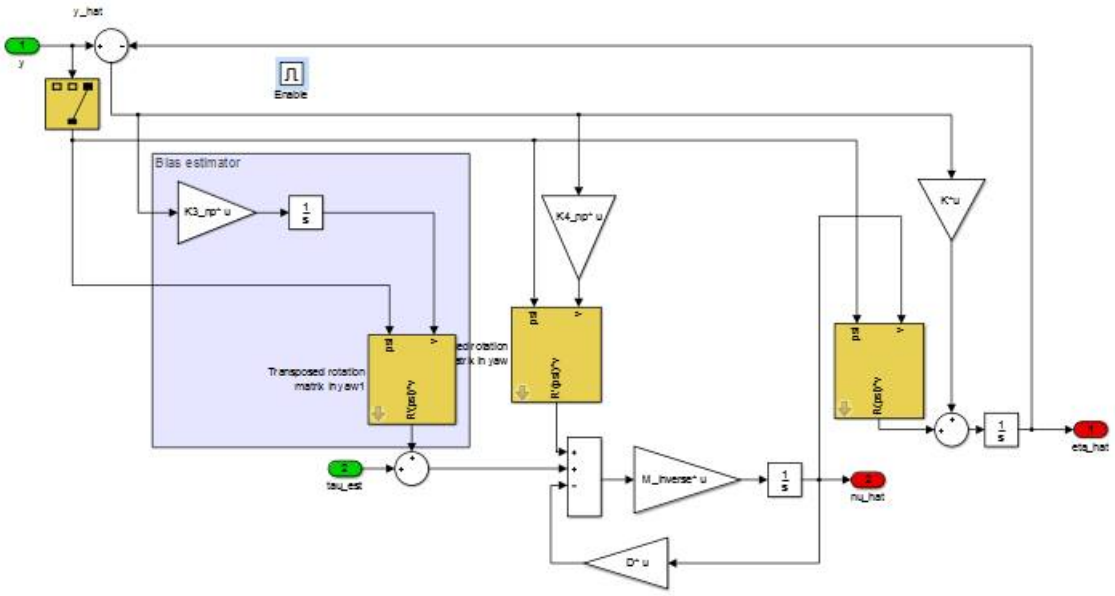

Figure 3.5: Nonlinear Passive Filter

Chapter 4

Thrust Allocation Implementation

In this chapter, thrust allocation implementation is discussed.

The most common thruster controlling method are speed control, pitch control, thrust control and power control. And in our case, we used thrust control, which indicates our control output in thrust allocation block are thrusts of five thrusters.

There are five thrusters on the vessel, the demonstration is as following in Figure 4.1

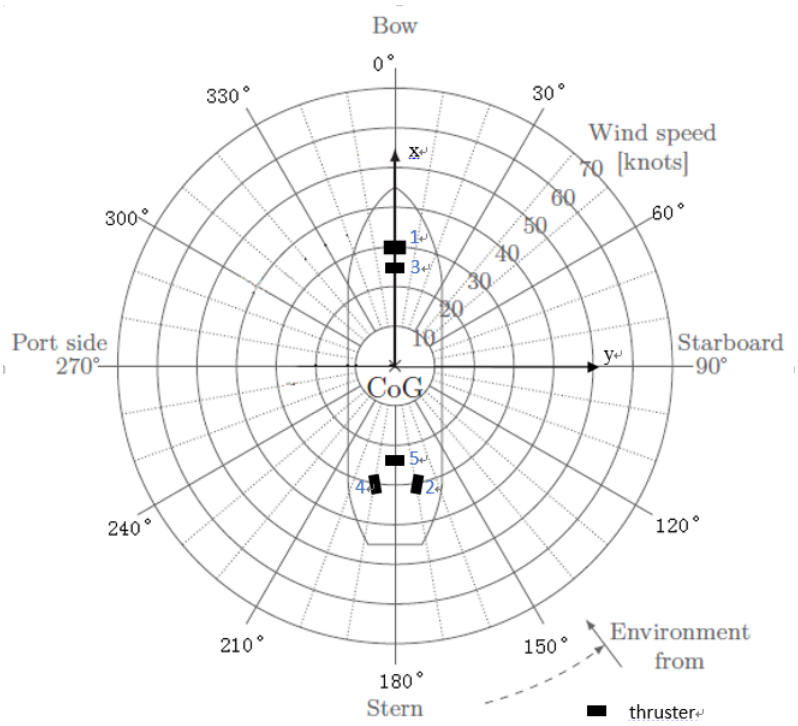

Figure 4.1: Sign Conventions

4.1 Desired Thrust τ

Desired thrust is the demanded loads from the DP controller and this will be translated to individual thrust set-point for each thruster by a thrust allocator.

τ is restricted to the motions in the horizontal plane of the vessel, leaving only surge, sway and yaw as degrees of freedom (these are controlled by the forces F_x,F_y and the moment M_z). The thrust allocator will be given the forces and moment required by the DP system. These are

defined as

$$\tau_d = [F_{x,d}, F_{y,d}, M_{z,d}]^T \tag{4.1}$$

4.2 Thruster Control Vector u

The state of each thruster is given by a thrust control vector u, and the thrust control vector in our case is the thrust of the thruster. All thrusters were given a fixed angle so they can be considered non-rotatable. The generated thrust is thus limited to a line shaped region. The maximal thrust were given by T_max in kN, which have already been implemented in "Thruster Dynamics" block.

4.3 Configuration Matrix

The configuration matrix is used to calculate the forces and moment on the ship, generated by thrust u. In our case, the center of gravity, CG, of the ship is assumed always set at the origin of our coordinate system. Thruster angle is given by α. Thus, for every thruster the forces and moment that it generates are given by

$$F_x = u \cdot cos(\alpha) \tag{4.2}$$

$$F_y = u \cdot sin(\alpha) \tag{4.3}$$

$$M_z = u \cdot (x \cdot sin(\alpha) - y \cdot cos(\alpha)) \tag{4.4}$$

The relationship between the thrust control vector u, configuration matrix $T_{3\times5}$ and the desired thrust τ_d is defined by

$$\tau_d = T_{3\times5}(\alpha) \cdot u \tag{4.5}$$

The thrust configuration matrix $T_{3\times5}$ is as following

$$T_{3\times5} = \begin{bmatrix} cos(\alpha1) & cos(\alpha2) & ... & cos(\alpha5) \\ sin(\alpha1) & sin(\alpha2) & ... & sin(\alpha5) \\ x_1sin(\alpha1) - y_1cos(\alpha1) & x_2sin(\alpha2) - y_2cos(\alpha2) & ... & x_5sin(\alpha5) - y_5cos(\alpha5) \end{bmatrix} \tag{4.6}$$

The x, y and α are provided for the five thrusters, and the configuration matrix is obtained by the given number. The figure 4.2 shows the result.

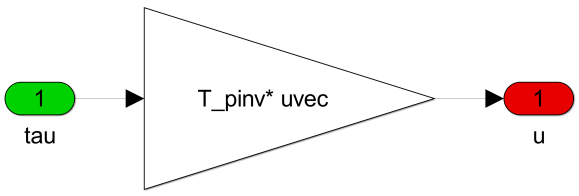

Figure 4.2: Thrust allocation

Chapter 5

Simulations

5.1 Simulation 1: Environmental loads

In simulation 1 the vessel are only influenced by the environmental loads, the current and wind. The current are coming from the East, with average speed $1\frac{m}{s}$, and the wind are coming form the North, with average speed $20\frac{m}{s}$.

What would be expected in this case is that the vessel position are moving in South-West direction. When it comes to the yaw one would turn smoothly until the wind and current are canceling each other. When it has reached this point it will oscillate according to the slowly varying. Figure 5.1 are showing this exact behavior.

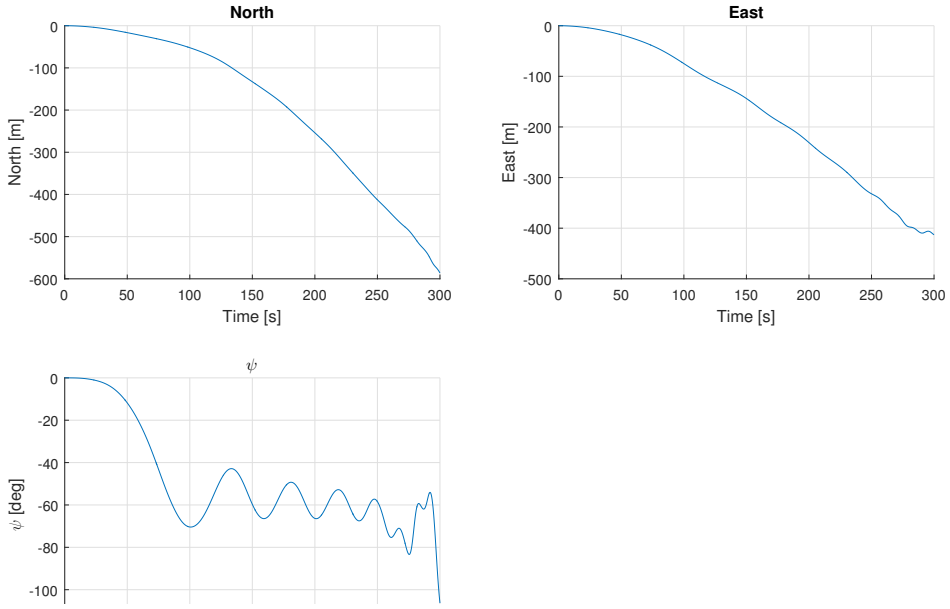

Figure 5.1: Position and atitude of the vessel

5.2 Simulation 2: DP and Thrust Allocation

In this simulation, we tested our DP controller and thrust allocator while environmental forces is excluded. The initial position is at the origin and the set point is at η_{SP}=[10m 2m pi/2]^T.

Firstly, we ran the simulation for the case where the thruster number 3 is not disabled. And

we get the plot of the vessel in NED frame for both actual position and the position from the reference model.

5.2.1 Simulation 2 with thruster 3

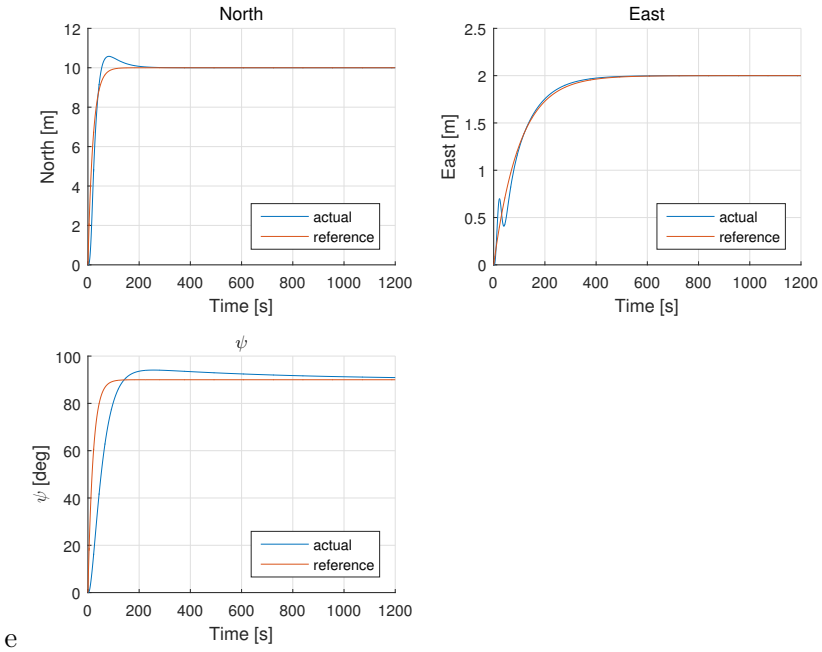

e

Figure 5.2: Vessel Position in NED Frame

It can be seen that in the north direction, the actual vessel position follows the position given by reference model well except that there is slight overshoot in the beginning in the actual position. In the east direction, it also performs well besides some small oscillation at the start. As for ψ, it takes much more time to reach the reference. It does not reach before 1200 s. The overshoot is around 5deg which is acceptable and there is also significant time-delay between the actual position and the one in reference model.

Later, we plot the desired force calculated by the DP controller, force setpoint for five thrusters and force applied by thruster dynamics block.

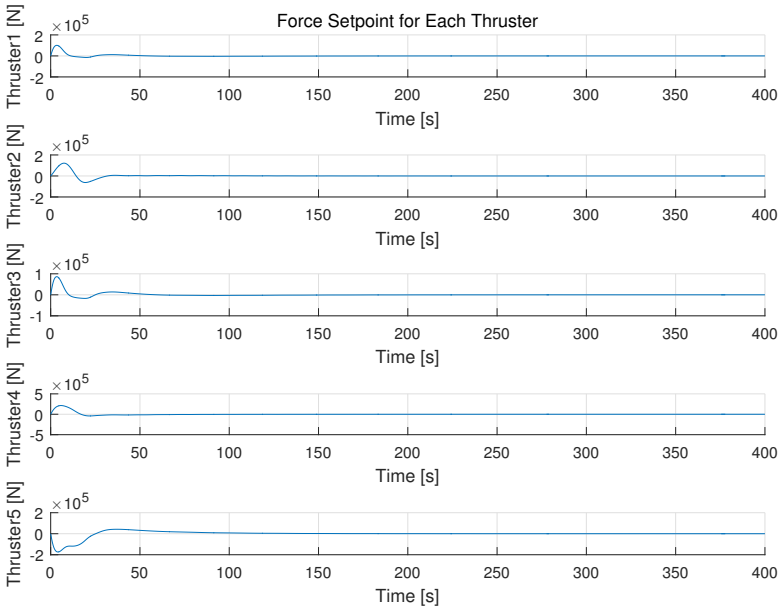

Figure 5.3: Force Setpoint for the Thrusters

It can be seen from figure 5.3 that during the first 50s, there are different force setpoints for different thrusters. It can be also told that thruster 4 and 5 is required to output large force and it is going to exceed the saturation value. And since thruster 5 locates close to the stern and have a degree of 90, the force setpoint is negative. However, after $t = 100s$, the force setpoint goes back to zero, which makes sense because the velocity to arrive the setpoint is achieved.

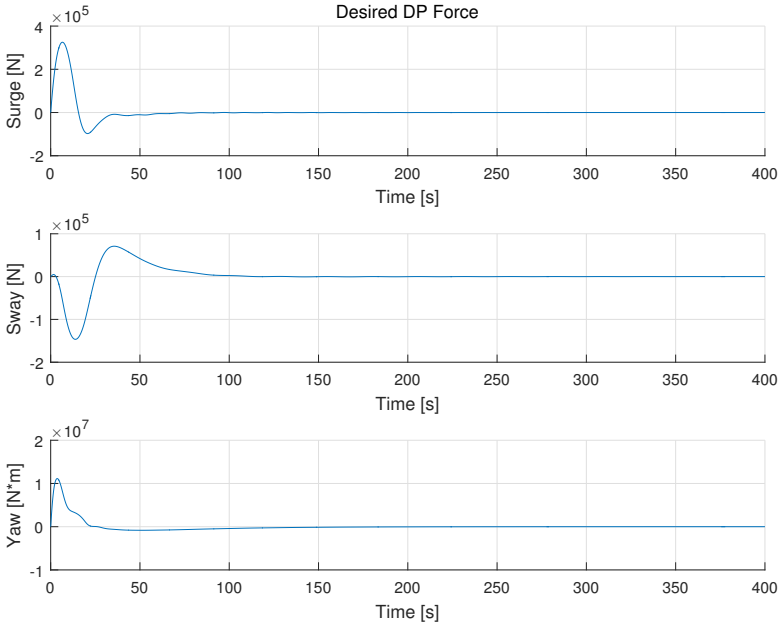

Figure 5.4: Desired Force Calculated by DP Controller

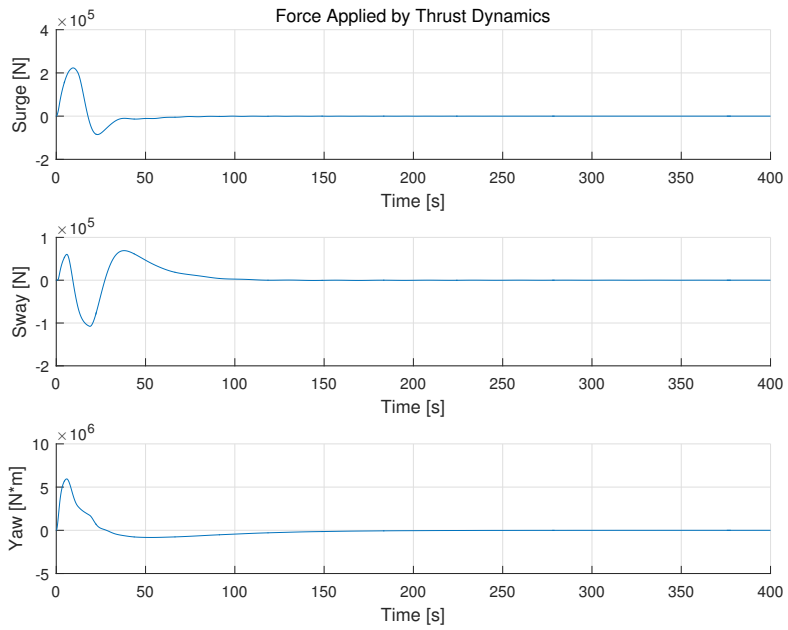

Figure 5.5: Force Applied by Thruster Dynamics Block

Compared the figure 5.4 and 5.5, the force applied by thruster dynamic block is smaller than the one desired by DP controller. This is reasonable because the saturation limitation works in the thruster dynamic block and give a saturated output force.

5.2.2 Simulation 2 without thruster 3

Then we simulated the same case but disabled thruster 3.

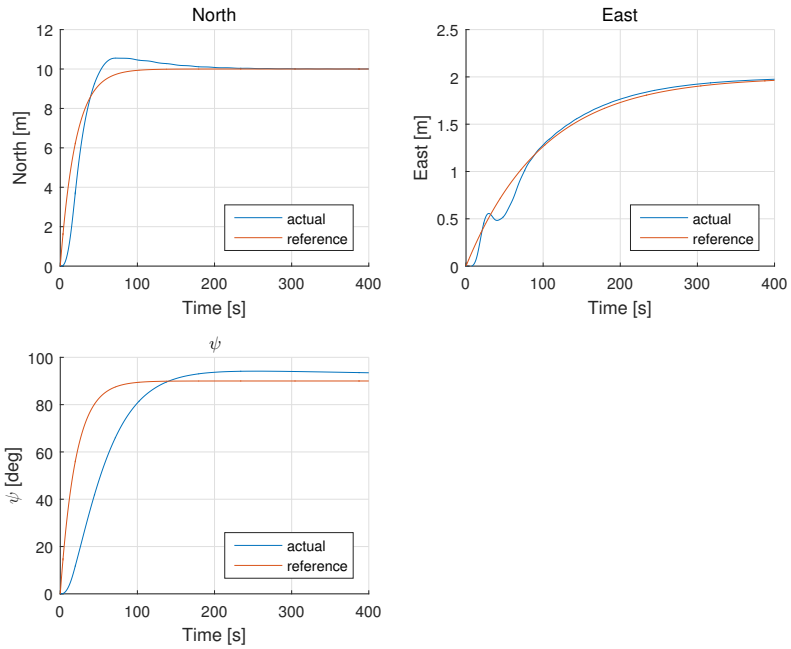

Figure 5.6: Vessel Position in NED Frame

It can be seen that in the north direction, the curve does not change. In the east direction, the small oscillation of the actual positio at the start becomes less significant. For ψ direction, it becomes a bit more slowly to reach the setpoint. It can be summarized that the system becomes slower and less robust towards the setpoint.

Later, we plot the desired force calculated by the DP controller, force setpoint for five thrusters and force applied by thruster dynamics block.

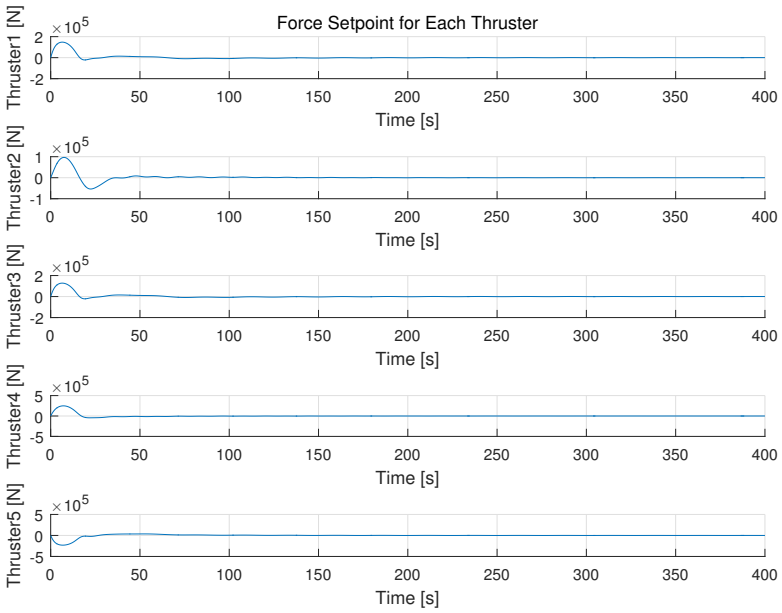

Figure 5.7: Force Setpoint for the Thrusters

It can be seen from figure 5.7 that the duration of the force outputs, when they are unequal to zero, last for a longer time duration, which is around 100s. Thruster 1, 4 and 5 is required to output large force and the values are going to exceed the saturation limit. Compared to the case with thruster 3, the force setpoint for thruster 1 and 5 becomes larger. Although thruster 3 is disabled, the allocator still gives setpoint to it and the setpoint is larger than the case with thruster 3. This can be explained as thruster 3 cannot contribute force anymore, the controller requires larger force from the thrusters to compensate.

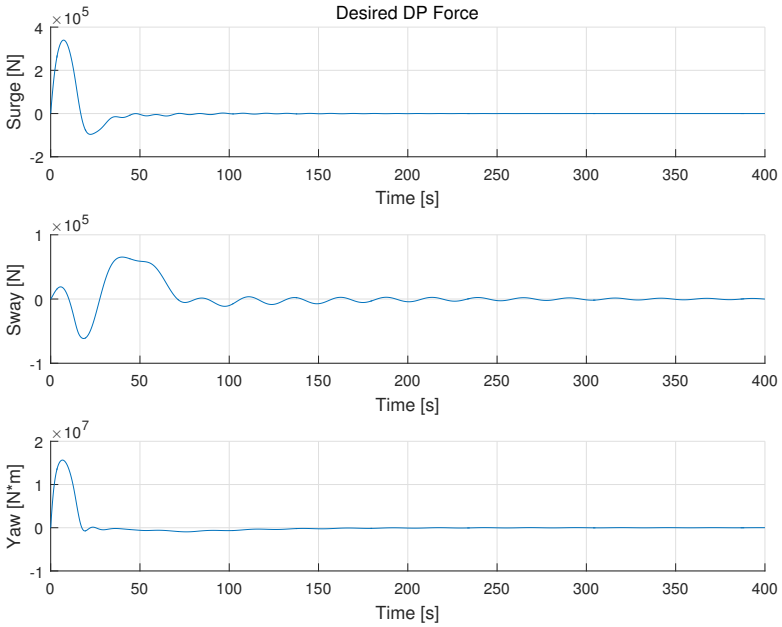

Figure 5.8: Desired Force Calculated by DP Controller

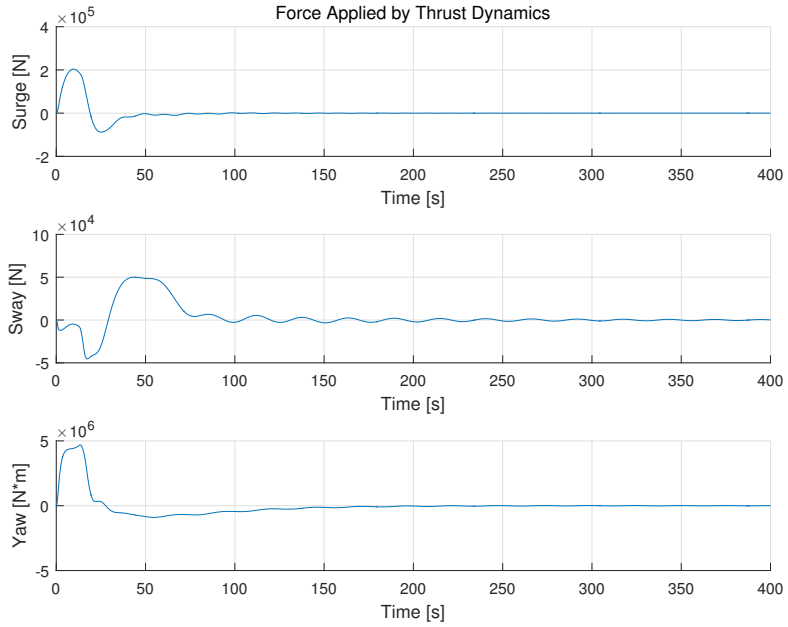

Figure 5.9: Force Applied by Thruster Dynamics Block

Compared, the figure 5.8 and figure 5.9, the force applied by thruster dynamic block is smaller than the one desired by DP controller. And there are more oscillations in curves of both plots, while the sway force and yaw moment from the thruster dynamic block is smaller than the case with thruster 3. It is also interesting to notice that the sway force output from the thruster dynamics block is negative at the beginning while it was positive at the start in the case with thruster 3. This is caused by no thrust output from thruster 3.

5.3 Simulation 3: DP and environment force

Compared to simulation 2, environmental forces from simulation 1 were now added. Due to not having noise involved yet, the observers are not used either. The initial setpoint was at the origin and the desired setpoint was set as η_{SP}=[10 2 $\frac{\pi}{2}$]^T. The response can be seen in figure 5.10.

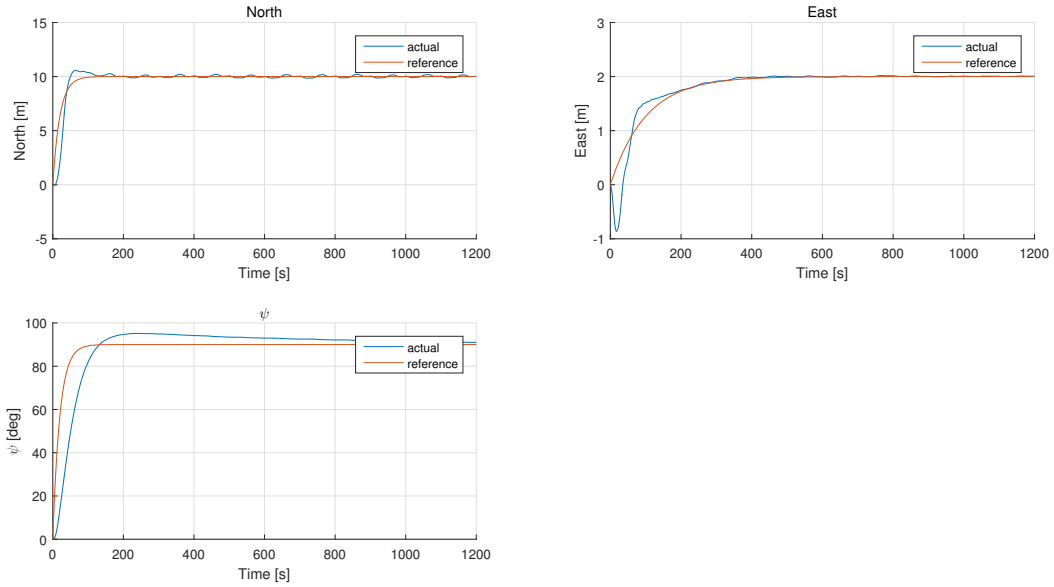

Figure 5.10: Vessel Position in NED Frame

As it can be seen in figure 5.10, when we inserted the environment forces to our system, the position of vessel acts differently than the the former simulation.

To be specific,in the north direction, DP system performed almost as well as before. The actual and the reference are quite identical. However, after the vessel arrived the setpoints, there was a slight oscillation while DP system trying to keep ship in the set point. It can be explained as the distraction caused by slow-varying and gust parts of wind. But amplitude is relatively tiny, which proved DP work in north direction to be good.

In the east direction, the DP system went first to west and then followed the reference. This can be due to the coupling with ψ, and we clearly see that the angle has some problem getting to reference compared to North. As mentioned in the first report, the ψ controller could have been tuned better, but due to the high gains and that we argued with it being satisfactory, we let the controller be the same as in the prior project. The vessel managed to stabilize it's position in the east to the reference quite well after around 300 seconds.

For the ψ direction DP system did not react not that quickly and even encountered a over-shot after 100 second,the results can still be acceptable, since at 1200 seconds the vessel has reached the reference point.

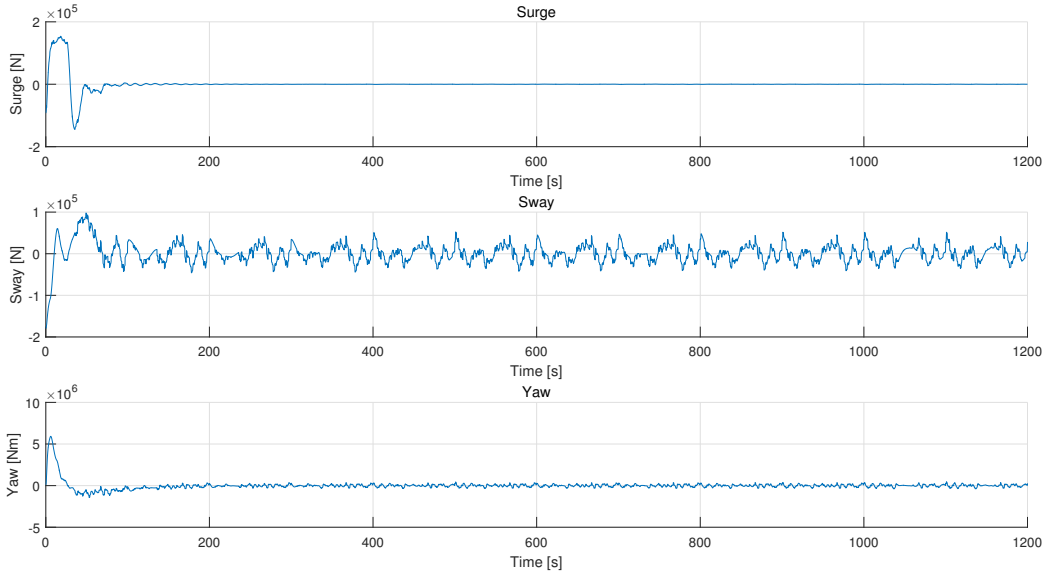

Figure 5.11: Sum of environmental and thruster forces/moment

Figure 5.11 shows the sum of the environmental and the thruster forces. As expected the sum is approximately zero when the desired set points are reached. That means the thrusters are able to counteract the forces and moment caused by the environment. That is what we were supposed to see. This means that the DP controller is tuned well enough and the trust allocation works. The thrusters are able to deliver the required forces and moment, in other words, they are not saturated.

5.4 Simulation 4: Observer selection

In this part, we tested two different observer designs by comparing the observer output with the real measurements before and after the noise is added to the signal. DP desired force is fixed at $\tau = [10^4 10^4 10^4]^T$.

5.4.1 Simulation with Extended Kalman Filter

When the noise block is disabled, the result vessel motion is shown in figure 5.12 and the vessel velocity is shown in figure 5.13.

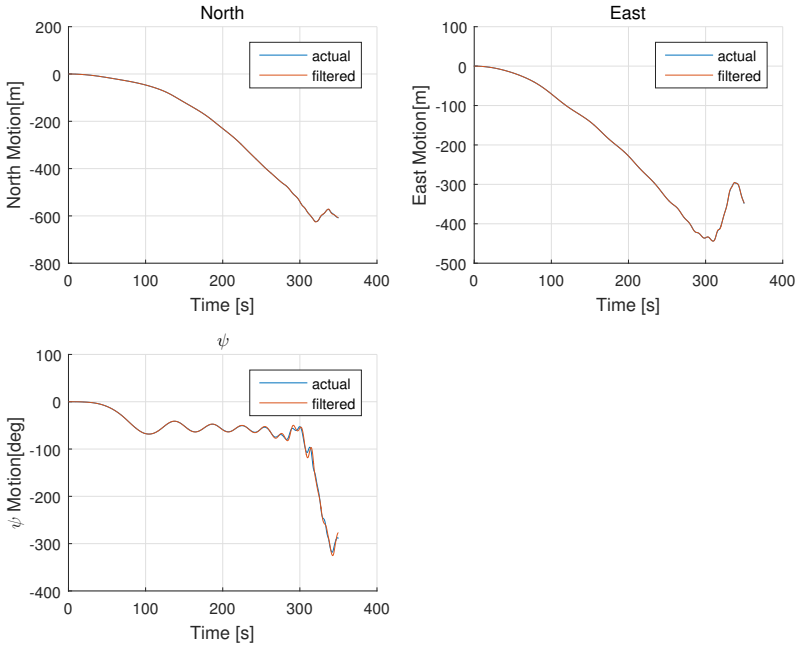

Figure 5.12: η without noise, EKF

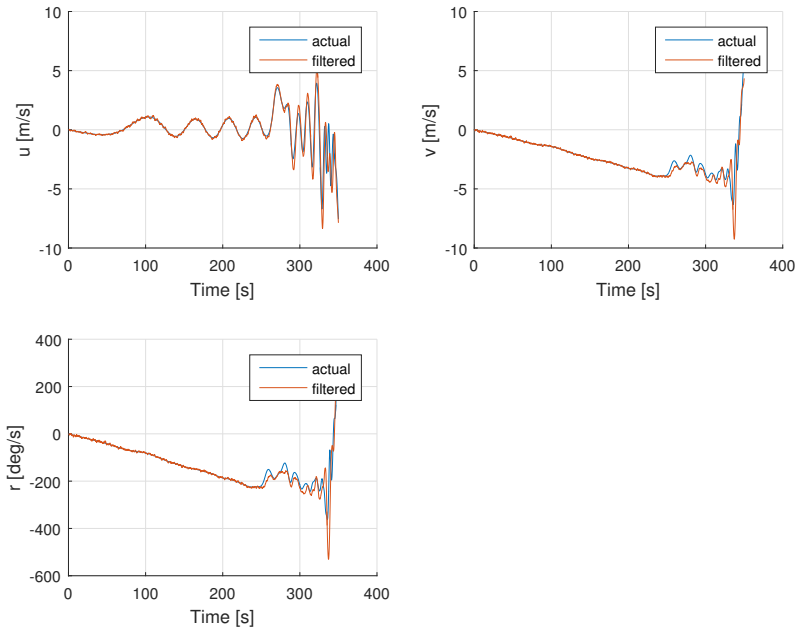

Figure 5.13: ν without noise, EKF

Figure 5.12 shows that the filtered vessel movement coincides well with the actual vessel movement, especially in North and East direction. While the velocity curves has larger deviation, particularly for velocities in East and ψ direction.

When the noise block is turned on, the result vessel motion is shown in figure 5.14 and the vessel velocity is shown in figure 5.15.

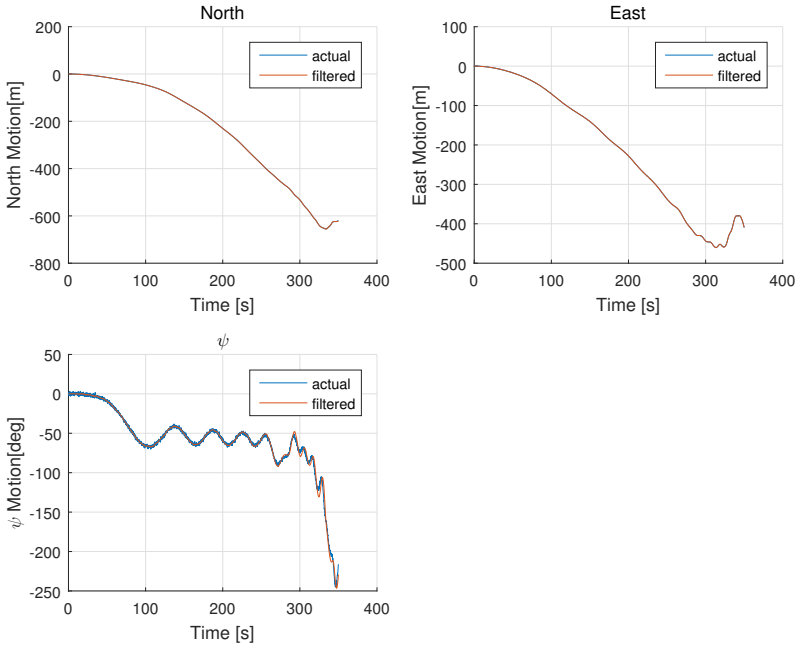

Figure 5.14: η with noise, EKF

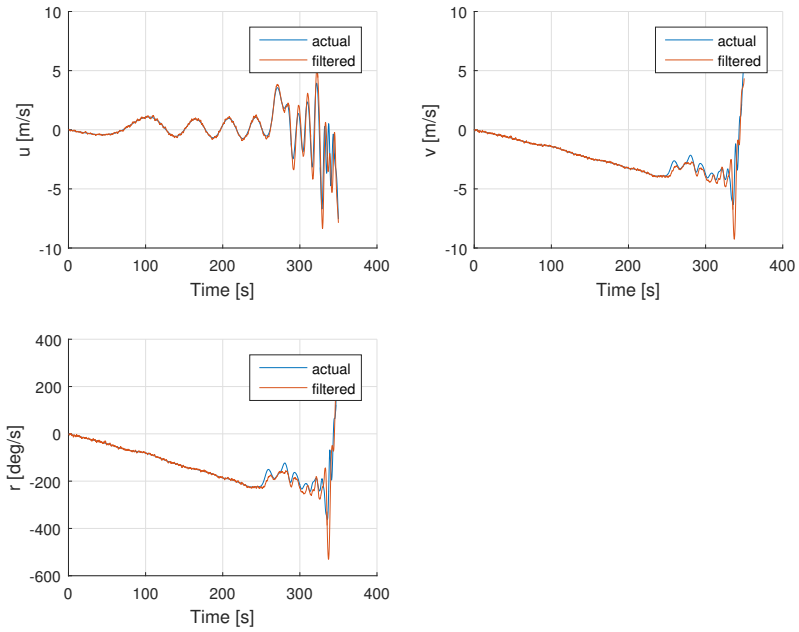

Figure 5.15: ν with noise, EKF

Since the noise magnitude is relatively low comparing to the vessel motion, the vessel motion with noise in the north and east direction look almost the same with the case where the noisy signal is disabled. The vessel motion in the ψ direction has small spikes. At the same time, the vessel velocities estimated by extended Kalman filter are spiky as well.

5.4.2 Simulation with Nonlinear Passive Filter

The same simulations were done for the Nonlinear Passive Observer (NPF) as well. These are shown in in figures 5.16-5.19.

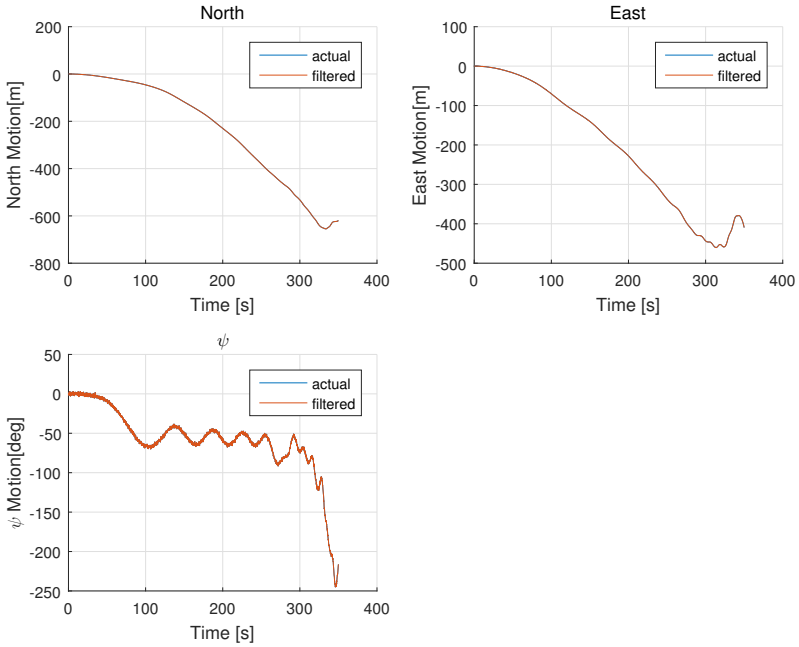

Figure 5.16: η without noise, NPF

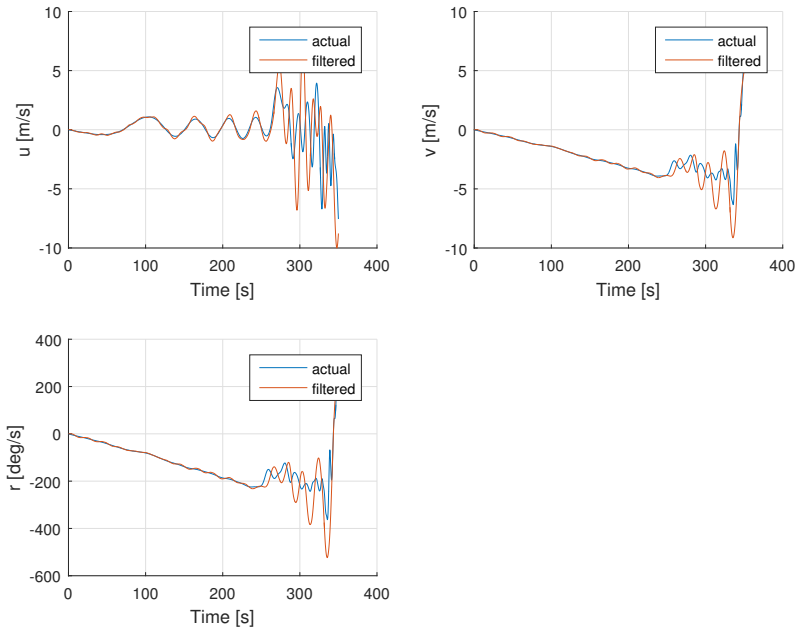

Figure 5.17: ν without noise, NPF

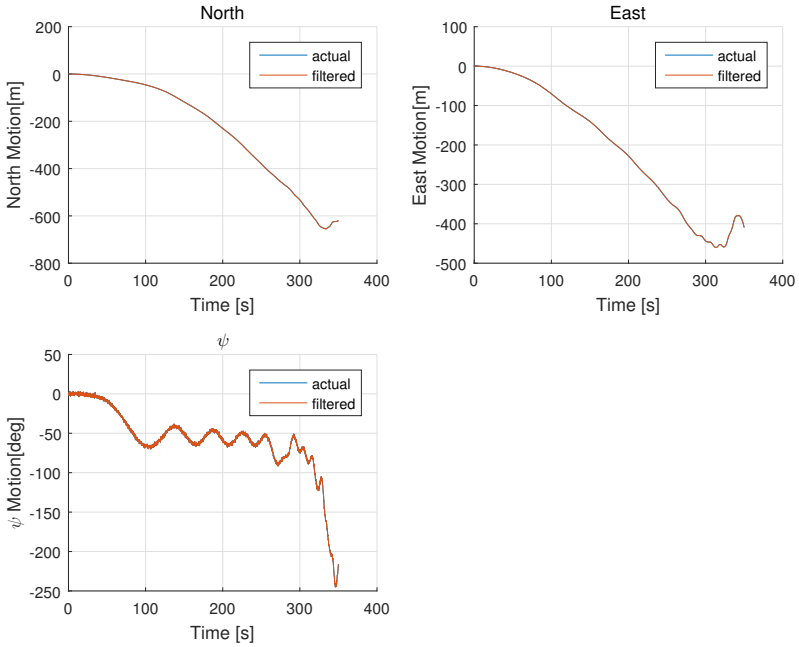

Figure 5.18: η with noise, NPF

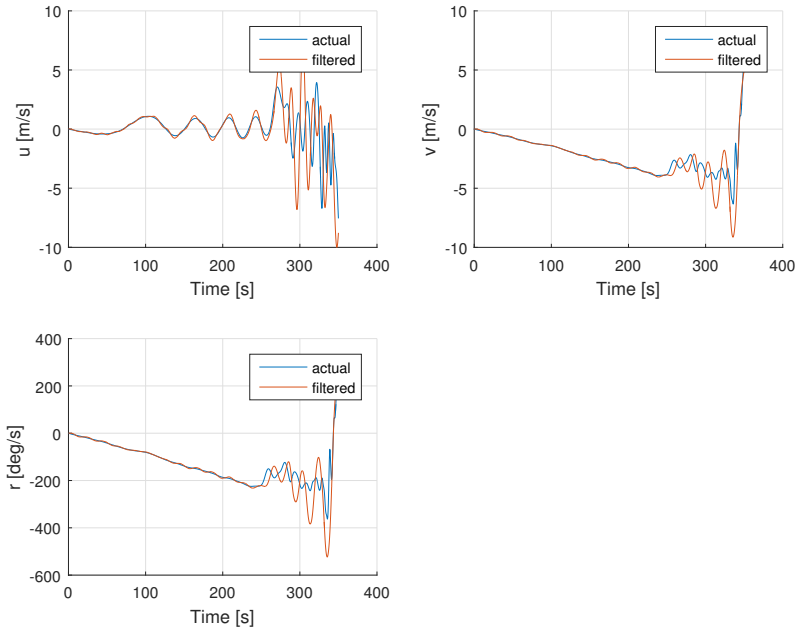

Figure 5.19: ν with noise, NPF

Which Observer to choose?

As expected the positions without noise is quite the same for both the EKF and NPF, but the velocity ν is estimated based on only positions measurement and forces. Thus we expected them to be somewhat different since EKF was more intuitively in this project that NPF due to the lack of waves. As mentioned prior we weighted the KYP lemma which gave us a bit worse velocity estimates for the NPF. Thus it is reasonable that the EKF in our case yielded a better estimate on velocity than NPF.

When the noise were turned on, the task of the observer is clearly seen. Both of them filtered the positions and gave estimates close to the actual signal (without noise). The velocity for both of the observers are quite good as well in the beginning. However in the end it can

clearly be seen that that the EKF is better.

Thus based on the observations above the EKF is a better tuned observer in our case.

5.5 Simulation 5: Complete simulation

This far the different parts of the total system have been examined one or two at a time. Now it is time to put every thing together. The wind are given to come from Northwest with mean velocity 15$\frac{m}{s}$. While the current are to come from Northeast with mean velocity 1$\frac{m}{s}$. As in the previous simulations the initial point is η =[0 0 0]. The setpoint, however, are now to be η_{SP}=[100m 50m pi/6]^T.

The first thing one can notice about this is that the vessel are to move a much longer distance than in the previous simulations. Therefore we have to give the reference model a larger time constant, to give the vessel enough time to reach the setpoint. Secondly one can look at how the desired heading angle are placing the vessel and see how the environmental forces are working on the vessel. The wind will give a negative force in surge, and positive in both sway and yaw. While the current are giving negative forces in all of them. This means that in sway and yaw the environmental forces to some degree will counteract each other and it may vary with one of them at the largest and then which direction the thrusters have to give thrust to get to or stay at the desired point. In surge, however, the environmental forces are only giving force in the negative direction. Then it is to expected that the thrusters have to give thrust to counteract this, pushing the vessel forward.

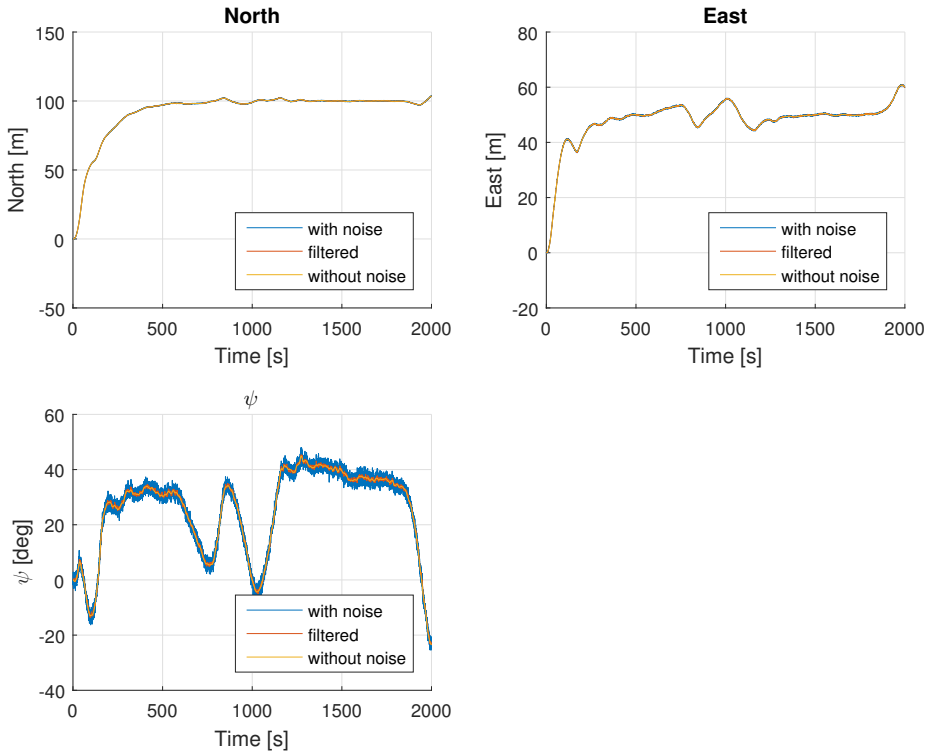

Figure 5.20: Position and orientation of the vessel in NED-frame

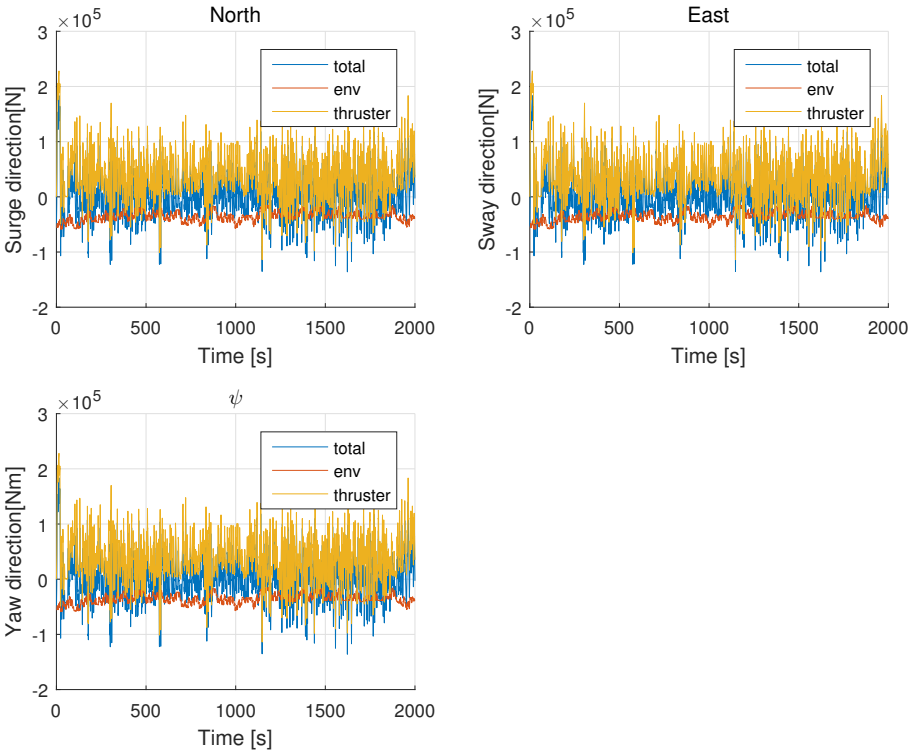

Figure 5.21: Forces acting on the vessel

Starting with the position in north direction, figure 5.20 shows that north is the one that fastest reaches and it is stable from the beginning. This makes sense since the north components of both wind and current are in the same direction. The east position, has more trouble with reaching and staying at the desired set point. Which also makes sense.

Looking at the yaw, it clearly are less stable. However if one compare it with the north and east positions the heading angle of the vessel give sense. From 600 s to almost 800 s the east position are increasing and the yaw decreasing. Then the east position goes steeply back again and the yaw likewise go steeply back. What we are seeing here are the thrusters giving a force in sway, which gives a moment in yaw do to the shape of the vessel - it is not made to move sideways. Therefore when the vessel are getting off the desired set position in east the vessel get some oscillations in east and yaw to get back to the desired setpoint.

In figure 5.21 the forces acting on the vessel. It is seen that the environmental forces are negative in all cases. In the beginning there are not possible to see a connection between the environmental forces and the thruster forces, this is before the vessel reaches the setpoint. After the vessel have reached the setpoint, the thruster forces are the same as the environmental forces, but positive. If we look specifically at the east direction around 600 s to 800 s, where the east position had some trouble. Looking closely it can be seen that the environmental forces are increased in this time area.

5.6 Simulation 6: Capability Plot

The vessel capability is tested for current of $U_c = 0m/s$, $U_c = 0.5m/s$, $U_c = 1m/s$ and $U_c = 1.5m/s$, while the vessel is capable to keep stable at origin at the maximum wind speed, and we tested it every 10 degrees. Assumed that the wind blows parallel to the current. And the obtained plot is shown below.

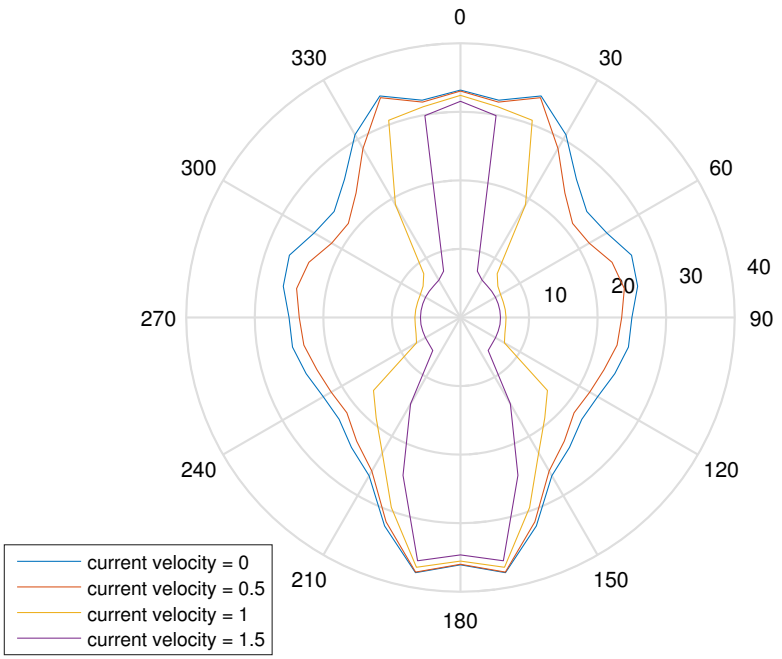

Figure 5.22: Capability Plots

As it can be seen from the figure, the maximum wind speed is the largest when it blows towards the vessel bow or stern, especially against bow. And the maximum wind speed becomes smaller when it blows towards the vessel board side. When the current velocity gets higher, the maximum wind speed at each angle has the trend of decreasing. Especially for two board sides of vessels, for instance, under the condition of current speed at 0.5m/s, this vessel could endure the wind at speed of 25m/s while the maximum speed ship could endure in right board side just slumped to only less than 10m/s. This could be explained as current coefficients increasing rapidly in two sides direction, so that current took up a large part of thruster forces and caused the decrease of ship's wind endurance. Adversely, in the directions of bow and stern, capability was not affected too much by current speed. Moreover, the capability plot is symmetrical on both sides of the vessel, which makes a good sense.

5.7 Simulation 7: Observer Robustness

As specified the vessel was kept at the initial condition and the position, η, and the velocity, ν, were plotted with the initial and the 10 times the initial noise power. To check the observer robustness we excluded the environmental forces such that the measurement noises were the only factor to affect the vessel.

The plots are given in figures (5.23-5.26).

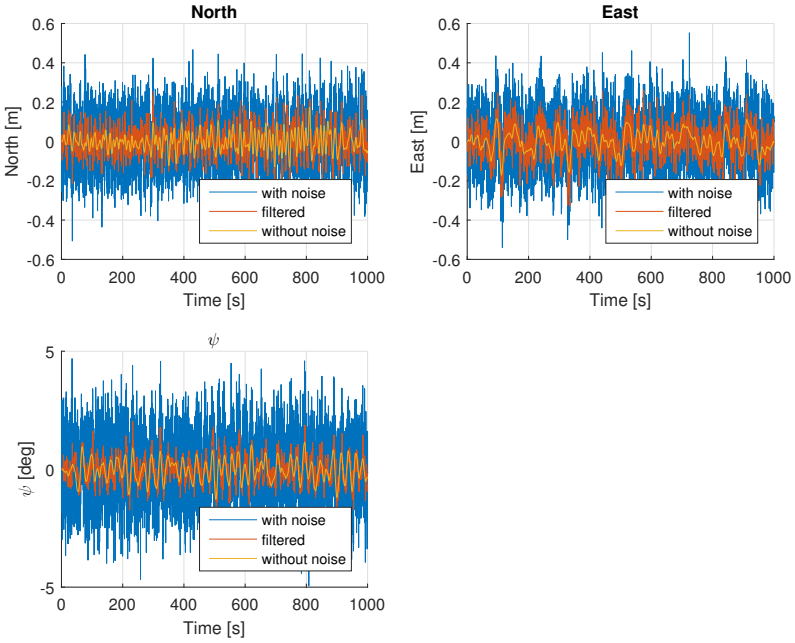

Figure 5.23: η with initial noise power

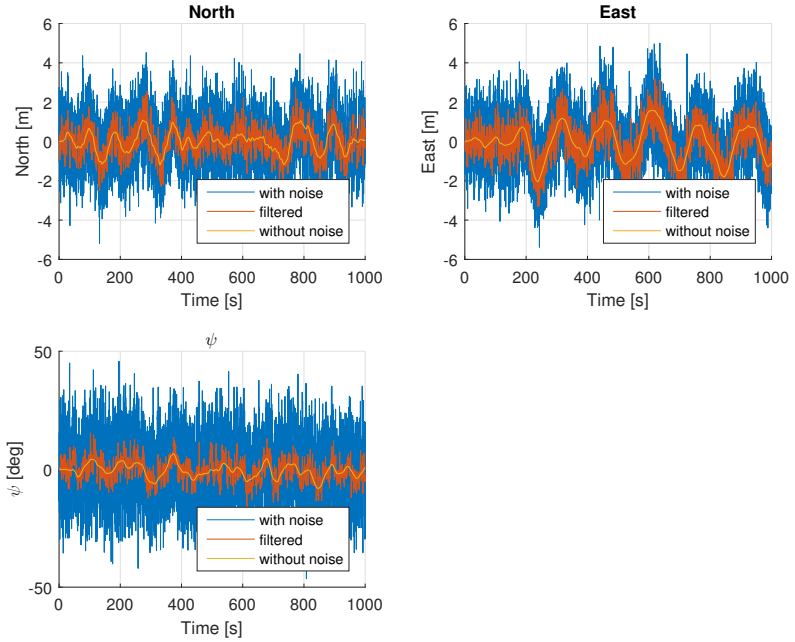

Figure 5.24: η with 10x initial noise power

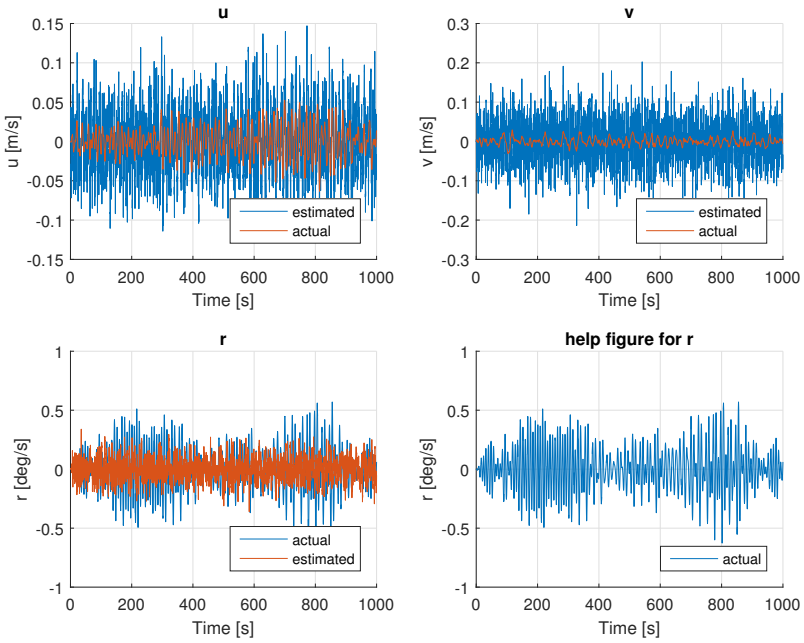

Figure 5.25: ν with initial noise power

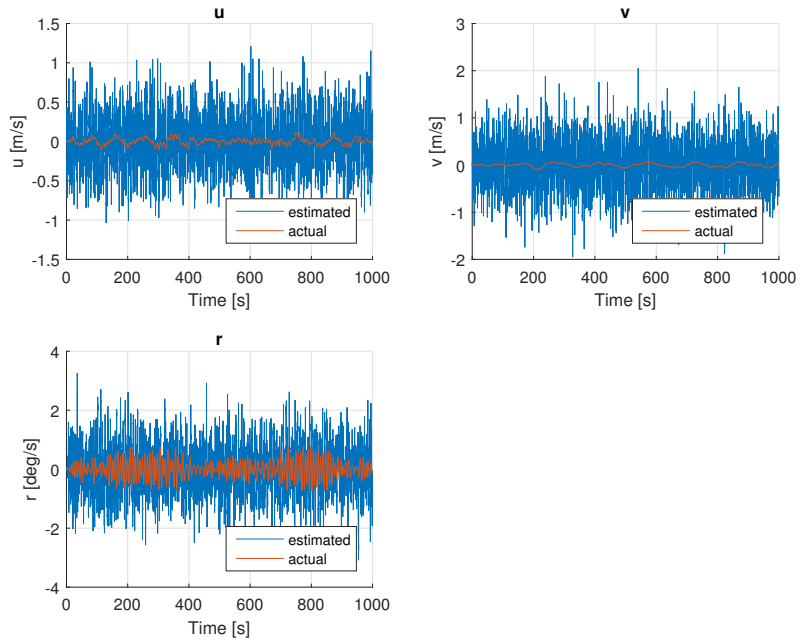

Figure 5.26: ν with 10x initial noise power

The figures 5.23 and 5.24 shows that the position of the vessel indeed is affected when the noise is increased by a factor of 10. In figure 5.24 in the East-direction the deviation after 200 seconds is around 3m from the desired position. In comparison the deviation at the same time in East in figure 5.23 ≈ 0. This arises a question that need to be answered before the robustness of the observer can be discussed. The question is: "How much deviation is acceptable when using so faulty sensors?

Since the faulty sensors would most probably in scenarios where better suited sensors are not applicable due to reasons, and those scenarios are more likely to be in the open sea and for a short duration, the deviation is not that much. It is acceptable.

The observer could have been tuned better, no doubt about that. However that is more dependent on what is satisfactory. In this project better estimates for velocity resulted in worse position. There was a trade-off and as seen in simulation 4, the accuracy in positions were weighted more than the accuracy for the velocity.

Note that the position in East was used as an example, it can clearly be seen that the noise is giving a similar characteristic in the North and ψ as well.

An other interesting part to look at is the the changes in the forces and moment the thrusters have to give as a result of the increased noise power. These can be seen in figures 5.27-5.29. The most interesting of those are figure 5.29 where the additional forces and moment are plotted. It can be seen that the forces and moment are quite high, they are almost identical to the forces and moment for the initial noise. This makes sense, since in this project the position is weighted as the most important. To have good position the DP-controller is trying to compensate for "almost everything". To have low power consumption (which relates to good estimates for velocity) and accurate position is hard with the setup of the Kalman filter implemented here. The tuning parameters of the observer will give a trade off.

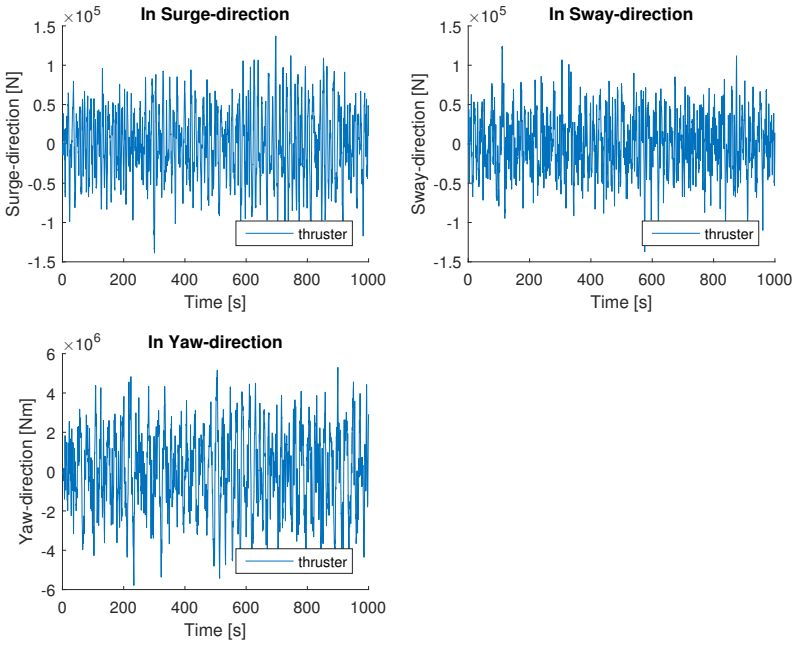

Figure 5.27: Thruster force and moment with initial noise power

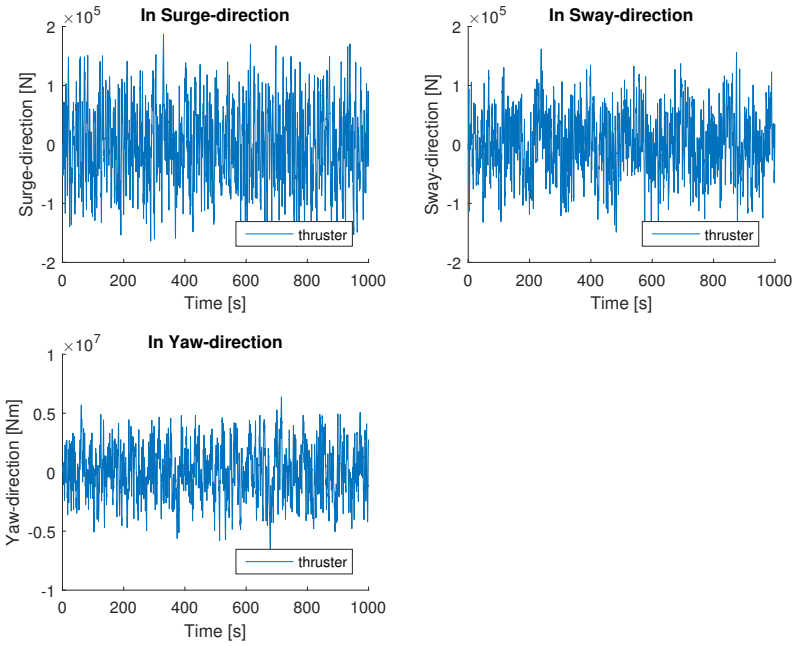

Figure 5.28: Thruster force and moment with 10x noise power

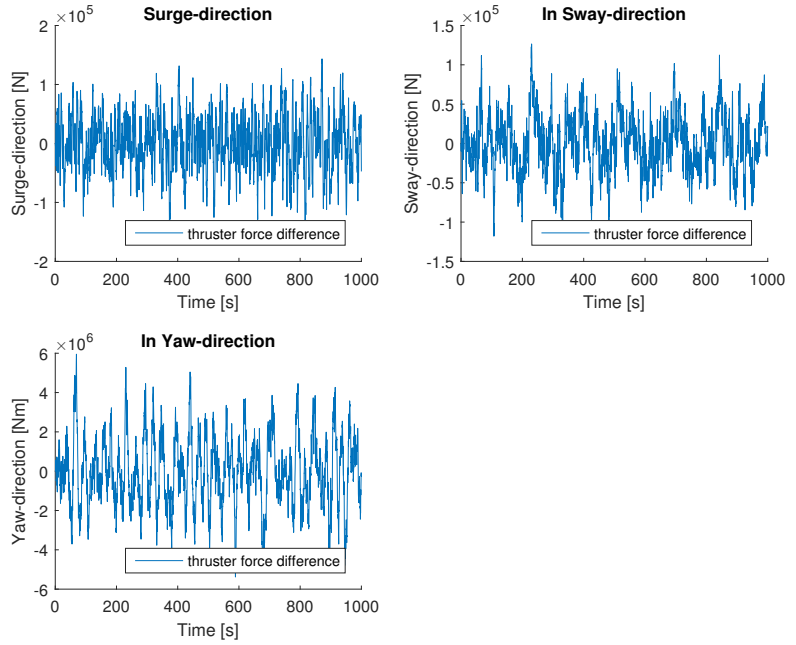

Figure 5.29: The difference in the thruster forces and moment, $\tau_{10x} - \tau_{1x}$

Based on the discussion above it is concluded that the observer is robust. The trust-usage is not a concern in this project and the deviations are acceptable.

Chapter 6

Summary

In the project part two, the forces working on the vessel have been made more realistic, both the environmental forces and the thrust forces. Two different observers have also been made and tested on the system. Also the positions, η, from the vessel have been given noise to make the scenarios more realistic. The different aspects of how it would be to control a vessel have been made much clearer than it was in the project part one. The thruster dynamics added in this part of the project have shown that it is not possible to give the desired control forces that the DP controller are giving, since in real life the thruster would have limits.

All in all this project has shown the importance of thrusters dynamic and allocation. It has shown what an observer is, how to implement it and most importantly why to use it. In addition more realistic environmental forces were shown and their importance. From the capability plot it can be seen how important the angle of the environmental forces are in order for the vessel to withstand it.

Bibliography

[1] T.I. Fossen. Handbook of Marine Craft Hydrodynamics and Motion Control. John Wiley & Sons, Ltd, 2011.

[2] Asgeir J. Sørensen. Marine Control Systems-Propulsion and Motion Control of Ships and Ocean Structures. Department of Marine Technology,NTNU., 2013.